Annals of Botany **122**: 605–615, 2018
doi: 10.1093/aob/mcy095, available online at www.academic.oup.com/aob

ANNALS OF BOTANY
Founded 1887

CO_2 and O_2 dynamics in leaves of aquatic plants with C_3 or CAM photosynthesis – application of a novel CO_2 microsensor

Ole Pedersen[1,2,*], Timothy D. Colmer[2], Emilio Garcia-Robledo[3,4] and Niels P. Revsbech[3]

[1]Freshwater Biological Laboratory, Department of Biology, University of Copenhagen, Universitetsparken 4, 3rd floor, 2100 Copenhagen, Denmark, [2]UWA School of Agriculture and Environment, Faculty of Science, The University of Western Australia, 35 Stirling Highway, Crawley, 6009 WA, Australia, [3]Microbiology, Department of Bioscience, Aarhus University, Ny Munkegade 114–116, 8000 Aarhus C, Denmark and [4]Ecology, Department of Biology, University of Cadiz, Poligono Rio San Pedro, 11510 Puerto Real, Cadiz, Spain
** For correspondence. E-mail opedersen@bio.ku.dk*

Received: 21 August 2017 Returned for revision: 9 April 2018 Editorial decision: 4 May 2018 Accepted: 7 May 2018
Published electronically 11 June 2018

• **Background and Aims** Leaf tissue CO_2 partial pressure (pCO_2) shows contrasting dynamics over a diurnal cycle in C_3 and Crassulacean Acid Metabolism (CAM) plants. However, simultaneous and continuous monitoring of pCO_2 and pO_2 in C_3 and CAM plants under the same conditions was lacking. Our aim was to use a new CO_2 microsensor and an existing O_2 microsensor for non-destructive measurements of leaf pCO_2 and pO_2 dynamics to compare a C_3 and a CAM plant in an aquatic environment.
• **Methods** A new amperometric CO_2 microsensor and an O_2 microsensor elucidated with high temporal resolution the dynamics in leaf pCO_2 and pO_2 during light–dark cycles for C_3 *Lobelia dortmanna* and CAM *Littorella uniflora* aquatic plants. Underwater photosynthesis, dark respiration, tissue malate concentrations and sediment CO_2 and O_2 were also measured.
• **Key Results** During the dark period, for the C_3 plant, pCO_2 increased to approx. 3.5 kPa, whereas for the CAM plant CO_2 was mostly below 0.05 kPa owing to CO_2 sequestration into malate. Upon darkness, the CAM plant had an initial peak in pCO_2 (approx. 0.16 kPa) which then declined to a quasi-steady state for several hours and then pCO_2 increased towards the end of the dark period. The C_3 plant became severely hypoxic late in the dark period, whereas the CAM plant with greater cuticle permeability did not. Upon illumination, leaf pCO_2 declined and pO_2 increased, although aspects of these dynamics also differed between the two plants.
• **Conclusions** The continuous measurements of pCO_2 and pO_2 highlighted the contrasting tissue gas compositions in submerged C_3 and CAM plants. The CAM leaf pCO_2 dynamics indicate an initial lag in CO_2 sequestration to malate, which after several hours of malate synthesis then slows. Like the use of O_2 microsensors to resolve questions related to plant aeration, deployment of the new CO_2 microsensor will benefit plant ecophysiology research.

Key words: Aerenchyma, Crassulacean Acid Metabolism, CO_2 microelectrode, leaf CO_2 and O_2, *Littorella uniflora*, *Lobelia dortmanna*, plant submergence, root radial O_2 loss, Severinghaus electrode, sediment O_2 consumption, shore-weed, underwater photosynthesis.

INTRODUCTION

CO_2 exchange of plant tissues with the environment is routinely measured using an infrared gas analyser (IRGA) with a leaf chamber and, together with measured stomatal conductance, the intercellular CO_2 concentration (c_i) can be estimated (Long and Bernacchi, 2003). The inferred tissue CO_2 partial pressure (pCO_2) may be checked by means of discrete sampling of tissue gases and subsequent analysis using IRGA or gas chromatography (GC) methods, but with the disadvantages of destructive sampling only at discrete times and with poor spatial resolution. In the present study, however, we used a new amperometric CO_2 microsensor with a linear response to external CO_2 (Fig. 1A, B) and a conventional O_2 microsensor (Revsbech, 1989) to elucidate with high resolution the CO_2 and O_2 dynamics within leaves of a C_3 and a CAM (Crassulacean Acid Metabolism) plant, in a comparative physiological study of these contrasting photosynthetic strategies as related to living submerged.

Leaf tissues of C_3 and CAM plants are expected to display contrasting patterns of CO_2 dynamics over a diurnal cycle and are thus well suited to demonstrate the CO_2 microsensor, and using this new technique to obtain continuous data on CO_2 acquisition by CAM vs. C_3 photosynthesis in aquatic plants. For C_3 plants, leaf tissue c_i has been estimated in many studies using an IRGA with an appropriate sample chamber. In the case of CAM plants, an IRGA cannot be used to estimate internal c_i since: (1) the stomata of most terrestrial CAM plants are closed throughout most of the light period; and (2) carboxylation of phosphoenolpyruvate (PEP) and de-carboxylation of malate can occur independently of stomatal conductance (Lüttge, 2004). Thus, studies on diurnal c_i dynamics have been limited to discrete samplings of tissue gases from CAM plants

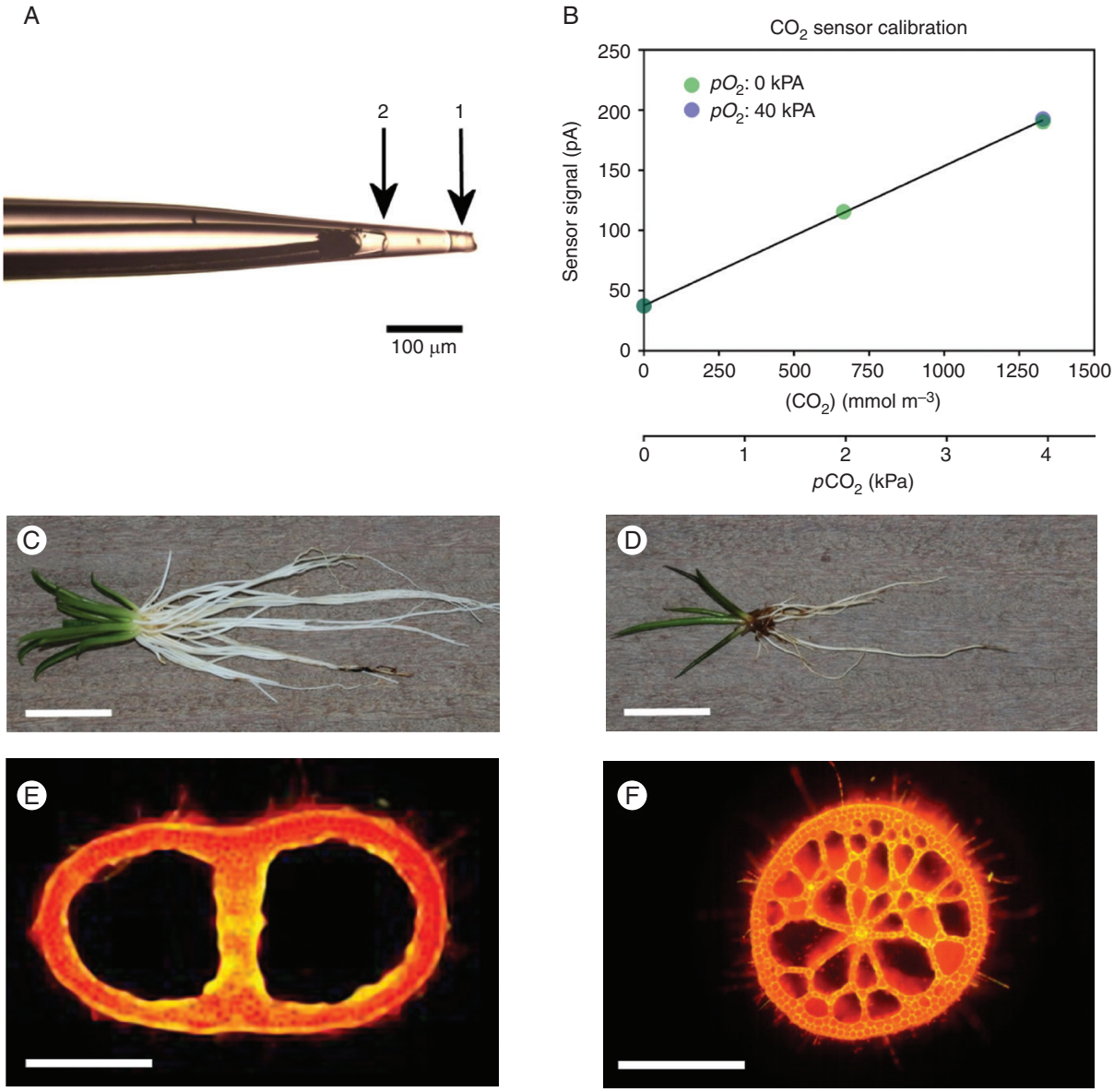

FIG. 1. Micrograph of the tip of the CO_2 microsensor used in the present study (A); Calibration curve of the CO_2 sensor (B); *Lobelia dortmanna* [whole plant (C); leaf cross-section (E)] and *Littorella uniflora* [whole plant (D); leaf cross-section (F)]; (E) and (F) were viewed using epifluorescence microscopy. In (A), arrow 1 indicates the silicone membrane of the tip (approx. 35 µm in diameter) of the CO_2 sensor and arrow 2 the tip of the CO_2 transducer positioned 130 µm behind the sensor tip. The small compartment between 1 and 2 contains the chemical O_2 scavenger (see the Materials and Methods). The CO_2 microsensor was calibrated in both the absence and presence (pO_2 = 40 kPa) of O_2 and showed no sensitivity to O_2 (CO_2 sensitivity = 39 pA kPa^{-1}, r^2 = 0.9999; B). The detection limit of the CO_2 sensor used was approx. 0.001 kPa. During measurements of tissue CO_2 and O_2, the microsensors were inserted into the leaf lacunae of *Lobelia dortmanna* (E, same lacuna for both the CO_2 and O_2 sensors) or 250 µm into the spongy leaf tissue of *Littorella uniflora* (F), in both cases <1 mm apart from each other. Scale bars in (C) and (D) = 2 cm; in (E) and (F) = 500 µm.

with bulky photosynthetic tissues (Spalding *et al.*, 1979; Kluge *et al.*, 1981). Moreover, many aquatic species lack functional stomata and in any case the leaves cannot be accessed with an IRGA leaf chamber when under water. In order to facilitate direct comparison under identical environmental conditions, we selected two submerged aquatic plant species which coexist and have relatively similar morphology and anatomy (both species are 'isoetids'; described in the next paragraphs) but with contrasting photosynthetic pathways; CAM and C_3 photosynthesis (Fig. 1C–F).

The vegetation of temperate carbonate-poor oligotrophic lakes is often dominated by isoetids, which are small inconspicuous plants of similar morphology deriving from convergent evolution. The isoetids share some unusual physiological traits as they all, to some extent, utilize sediment-derived CO_2 for photosynthesis in the shoot (Wium-Andersen, 1971; Raven *et al.*, 1998). This rather unusual strategy is due to the carbonate-poor water containing little inorganic carbon, whereas CO_2 derived from mineralization tends to accumulate in the interstitial water of the sediment (Pedersen and Sand-Jensen, 1992;

Pedersen *et al.*, 1995, 2011*a*). CO_2 enters the relatively large unbranched root system by radial CO_2 gain (RCOG) and diffuses to the leaves via the extensive aerenchyma that enables fast gas phase diffusion along the plant organs. Once in the leaves, CO_2 is not lost to the water column by radial CO_2 loss (RCOL) since the leaves possess a cuticle of relatively high resistance to gases (Møller and Sand-Jensen, 2012), a trait which is rare amongst aquatic plants (Sculthorpe, 1967; Hutchinson, 1975). As a consequence, O_2 produced in photosynthesis is hardly lost to the water column but instead follows the same, but in the opposite direction, low resistance route into the roots where a large proportion of O_2 enters the sediment by root radial O_2 loss (ROL), a process common in most wetland plants albeit with markedly different spatial patterns of ROL along roots (Armstrong, 1964, 1979; Colmer, 2003). This specialized physiology leads to distinctive diurnal cycles of CO_2 and O_2 in sediments inhabited by isoetids (Pedersen *et al.*, 1995; Lenzewski *et al.*, 2018).

Lobelia dortmanna L. (water lobelia) is probably the most studied of all isoetids, and the characteristic carbonate-poor lakes inhabited by this species are often referred to as 'lobelia lakes'. *Lobelia dortmanna* is a C_3 plant (Maberly and Spence, 1983; Farmer and Spence, 1985), and during the light period under conditions with high CO_2 and low O_2 around the roots and low CO_2 and high O_2 in the water column, close to 100 % of the gas exchange takes place across the roots (Sand-Jensen and Prahl, 1982). As a consequence of the relatively impermeable leaves, O_2 for night-time respiration is taken up from the sediment that can remain oxic due to the low O_2 consumption rate within this substrate (Table 1; Pedersen *et al.*, 1995; Sand-Jensen *et al.*, 2005).

Littorella uniflora (L.) Aschers. (shore-weed) often grows intermingled with *Lobelia dortmanna*, but *Littorella uniflora* is a CAM plant (Madsen, 1985). CAM photosynthesis is a common trait among isoetids where it does not serve to conserve water, but rather to sequester free CO_2 (Keeley, 1998). In the carbonate-poor waters, inorganic carbon is a scarce resource, and the ability to take up CO_2 deriving from tissue as well as community respiration during the night is thus a competitive advantage (Keeley and Busch, 1984). Indeed it has been suggested that CAM photosynthesis first evolved in aquatic plants (the genus of *Isoetes*) as a carbon-concentrating mechanism (Keeley, 1998). However, *Littorella uniflora* also takes up sediment-derived CO_2 for photosynthesis during the day, but, since the leaf cuticle is more permeable than that of *Lobelia dortmanna* (Møller and Sand-Jensen, 2012), a greater fraction of the O_2 produced by photosynthesis diffuses to the water column, decreasing the amount which moves via the roots and into the sediment (Sand-Jensen *et al.*, 1982). The morphology of *Littorella uniflora* is relatively similar to that of *Lobelia dortmanna* (Madsen and Sand-Jensen, 1991); both species have short stiff leaves arranged in a rosette and an extensive unbranched root system, and both organs are of high gas-filled porosity (Fig. 1E, F).

In the present study, we aimed to elucidate and compare the pCO_2 and pO_2 dynamics within intact leaves of plants with contrasting photosynthetic pathways (C_3 vs. CAM), using non-destructive measurements by microsensors with high spatial and temporal resolutions. For the aquatic C_3 plant, we hypothesized that in light the leaf pCO_2 would decline and pO_2 would increase due to the impermeable leaf cuticle, whereas in darkness CO_2 would accumulate and O_2 would be depleted. For the aquatic CAM plant, we hypothesized that in light the leaf pCO_2 would also decline but with some influence from CO_2 produced from the de-carboxylation of stored malate, and, as with the C_3 plant, we expected that the leaf pO_2 would increase owing to photosynthesis. In darkness, however, we hypothesized that leaf pCO_2 in the CAM plant would remain relatively low due to conversion into malate, as compared with CO_2 in the C_3 plant, whereas leaf pO_2 was expected to decline in the CAM plant similarly to that in the C_3 plant.

Table 1. *Summary of* Lobelia dortmanna *(C_3) and* Littorella uniflora *(CAM) leaf tissue* pCO_2 *and* pO_2 *and sediment* pCO_2 *and* pO_2 *extracted from Figs 2–5 and Supplementary Data Figs S1 and S2*

		Lobelia dortmanna (C_3)	*Littorella uniflora* (CAM)	Sediment
Light	pCO_2 (kPa)	Below the detection limit	0.3	Approx. 2
	pO_2 (kPa)	21	25–30	8–18
Dark	pCO_2 (kPa)	2.5–3.5	<0.05	Approx. 5
	pO_2 (kPa)	<0.2	10–15	0–10

The summary provides ranges of quasi-steady state values towards the end of the light or dark periods in both leaf tissues and sediment, at 20 °C. Information on the number of replicates is available in the respective figure legends. The biological O_2 consumption (nmol L^{-1} sediment s^{-1}) of the sediment was 19.4 ± 0.83 (mean ± s.e., n = 5), and sediment organic matter (% w/w) was 0.74 ± 0.03 (mean ± s.e., n = 5).

MATERIALS AND METHODS

Plant material

Vegetated turfs with mixed populations of *Lobelia dortmanna* L. (C_3 photosynthesis) and *Littorella uniflora* (L.) Aschers. (CAM photosynthesis) were collected from the littoral zone of Värsjön, Skåne, Sweden (56.321755°N, 13.489416°E) in April 2016. Each turf was approx. 500 cm^2, 15–20 cm deep and had densities of approx. 500 individuals m^{-2} for *Lobelia dortmanna* and approx. 3000 individuals m^{-2} for *Littorella uniflora*. The sediment was sandy and with a low concentration of organic matter, and thus also low biological O_2 consumption (Table 1). The turfs were placed in aquaria with artificial lake water diluted to 10 % of that described by Smart and Barko (1985) and with a carbonate alkalinity of 50 mmol m^{-3} to mimic the water composition of the lake habitat. The turfs were illuminated by fluorescent light (TL-D deLuxe 965, Philips, Amsterdam, The Netherlands) providing a photon flux density of about 200 µmol photons m^{-2} s^{-1} in a 14 h light and 10 h dark cycle at 20 °C. The water column was bubbled with atmospheric air to keep the water at near air equilibrium (approx. 284 mmol O_2 m^{-3} and 16 mmol CO_2 m^{-3}). The turfs were always submerged and were allowed to acclimate to these environmental conditions for a minimum of 10 weeks.

Sensor principles and calibration

In contrast to CO_2, Clark-type O_2 microsensors have long been available to plant scientists, enabling continuous measurements

of tissue O_2 with high temporal and spatial resolution (Clark, 1956; Armstrong, 1979; Revsbech, 1989). CO_2 microsensors of the Severinghaus type (Severinghaus and Bradley, 1958) are available, but these are based upon indirect measurements of CO_2 via changes in pH using a pH-sensitive transducer embedded in a small reservoir with bicarbonate and carbonic anhydrase (CA) to speed up hydration of CO_2 (Caflisch *et al.*, 1979; De Beer *et al.*, 1997; Zhao and Cai, 1997). Due to the pH-sensitive transducer, these sensors are sluggish and respond to external CO_2 in a logarithmic fashion with poor resolution at high CO_2 concentrations.

In the present study, leaf tissue CO_2 and O_2 were measured using custom-built microsensors. The novel CO_2 microsensor with a tip diameter of 35 µm consisted of an outer casing sealed at the very tip with a gas-permeable silicone membrane (Fig. 1A). Behind the membrane, there was a reservoir holding a chemical O_2 scavenger (1 mol $CrCl_2$ L^{-1} in 0.1 mol HCl L^{-1}) to prevent O_2 interference with CO_2. The tip of the CO_2 transducer was positioned within the outer casing about 80 µm behind the outer membrane. The microsensor was polarized at –1.2 V and had a linear response to CO_2 in the external medium up to at least 1400 µmol L^{-1} (4 kPa), and was insensitive to O_2 (Fig. 1B). When the microsensor was not used, the tip was stored in an alkaline ascorbate solution (zero O_2 and CO_2; see calibration of O_2 microsensor) to keep the zero current low and to extend the life time of the chemical O_2 scavenger.

Calibrations of the CO_2 microsensor were carried out at 20 °C at three different CO_2 concentrations in artificial lake water (always at 10 % concentration; for composition see 'Plant material') of low and high pO_2 to check possible interference from O_2. A calibration solution of zero CO_2 and zero O_2 was obtained by bubbling the artificial lake water without any inorganic carbon added and at pH >11 with high purity N_2 for 1 h; at high pH, all inorganic carbon is converted into CO_3^{2-} (although inorganic carbon was not added to the solution, it might still have dissolved from atmospheric air) and the N_2 removes (purges out) dissolved O_2 and also CO_2. A solution with zero CO_2 but with approx. 40 kPa pO_2 was obtained by mixing solutions purged with high purity N_2 or O_2 and adjusted to pH >11. Calibration solutions with either zero O_2 or approx. 40 kPa pO_2 but with a CO_2 concentration of about 700 or 1400 µmol L^{-1} (corresponding to approx. 2085 and 4071 Pa pCO_2) were prepared by injecting known amounts of $KHCO_3$ into acidified (pH <2 using HCl) artificial lake water prepared as above. The CO_2 microsensor used in the present study did not show any interference with O_2 within the range tested (0–40 kPa pO_2, Fig. 1B). The CO_2 microsensor was calibrated prior to each experiment, and calibration and O_2 sensitivity were again checked after each experiment, at 24–30 h after the first calibration depending on the experimental design. If calibrations before and after measurements differed, corrections were performed by assuming linear drift in signal over time.

The O_2 microsensor (tip diameter = 25 µm) used for tissue O_2 measurements was constructed according to Revsbech (1989) and polarized at –0.8 V. It was calibrated at zero O_2 (approx. 2 g of ascorbate in 100 mL of deionized H_2O in 0.1 N NaOH) and at air equilibrium (284 mmol O_2 m^{-3} at 20 °C, corresponding to 20.6 kPa pO_2). The sensor has previously been shown to respond linearly to O_2 up to 101 kPa pO_2 (Revsbech, 1989).

The CO_2 and the O_2 microsensors were connected to a picoampere meter (Field Multimeter, Unisense A/S, Denmark) and the sensor signals were collected with a frequency of one sample per minute using data acquisition software (SensorTrace Suite 2.8, Unisense).

Leaf tissue and sediment measurements of CO_2 and O_2

The CO_2 and O_2 microsensors were each mounted on separate micromanipulators (MM35, Unisense) and rotated to an angle which enabled insertion of both microsensors into the same leaf, with the tips <1 mm apart. In the case of *Lobelia dortmanna* (n = 2; different individual plants in different turfs), the two microsensors were furthermore simultaneously positioned with tips into the same leaf lacuna (see cross-section in Fig. 1E), whereas in *Littorella uniflora* (n = 3; different individual plants in different turfs) the two microsensors were positioned with tips simultaneously approx. 250 µm into the spongy leaf tissue (see cross-section in Fig. 1F); in both species, the microsensors were inserted about one-third of the way along the leaf down from the tip (10–20 mm from the tip). During measurements, the entire turf remained submerged and was evenly illuminated (14 h) with cool LED light (ALCX3100, Ceab Acquari, Brescia, Italy) providing a photon flux density of about 200 µmol photons m^{-2} s^{-1} at canopy height, or kept in complete darkness (10 h). The turf was kept in a constant temperature bath (20 °C) and the water column was bubbled with atmospheric air to maintain near air equilibrium of CO_2 (16 mmol m^{-3}) and O_2 (284 mmol m^{-3}) in both light and darkness.

Following successful measurements of tissue CO_2 and O_2 dynamics, sediment CO_2 (n = 2) dynamics were followed over a diurnal period by inserting the CO_2 microsensor approx. 30 mm into the sediment where the root density is high (Pedersen *et al.*, 1995) and was about 20 mm away from the nearest plant; the distance to the nearest root was unknown. Sediment pO_2 was measured (n = 10) using commercially available needle-embedded O_2 optodes (OXF500PT, Pyro Science GmbH, Aachen, Germany) connected to a REDFLASH meter (MicroOptode Meter, Unisense) and the signal was collected with a frequency of one sample per minute using data acquisition software (SensorTrace Suite 2.8, Unisense). The O_2 optodes were calibrated in the same way as described for the O_2 microsensor. All calibrations, like the measurements, were at 20 °C.

In one case (n = 1), the dark period was extended by 2 h (12 h in total) in order to test the effect upon tissue and sediment CO_2 and O_2 responses.

Leaf tissue organic acids

Leaves of *Lobelia dortmanna* and *Littorella uniflora* were sampled at the end of the dark or light periods. The achlorophyllous basal parts were trimmed off and discarded, since such tissues have previously been shown to be insignificant for accumulation of organic acids (Pedersen *et al.*, 2011*b*). The leaves were immediately frozen in liquid N_2 and then freeze-dried. The samples were ground in a ball mill, and a weighed sub-sample was then extracted in ice-cold 5 % (v/v) perchloric acid (Fan *et al.*, 1993). The extract was mixed well using a

vortex and then centrifuged at 11 800 *g* for 30 min at 4 °C, after which the supernatant was collected and the pellet was again extracted in ice-cold 5 % perchloric acid. The supernatants of both extractions were combined and pH adjusted to 3.0–3.5 using K_2CO_3 to precipitate the perchlorate, while always on ice. The sample was centrifuged (as above) and the supernatant collected, and the volume was measured to enable calculation of organic acids in the extracted tissues. The extracts were frozen (–18 °C) until they were analysed by high-performance liquid chromatography (HPLC; 600E pump, 717+ autoinjector, 996 photodiode array detector; Waters, Milford, MA, USA) following the method described in detail by Pedersen *et al.* (2011*b*).

Underwater net photosynthesis and dark respiration

Underwater net photosynthesis (P_N) or dark respiration (R_D) was measured based on O_2 evolution or consumption by tissues in a sealed glass vial following the approach of Pedersen *et al.* (2013). In brief, leaves (n = 4 or 5) of both *Lobelia dortmanna* and *Littorella uniflora* were excised just above the achlorophyllous basal parts (i.e. green tissues only) and then sliced longitudinally in half to expose the inner tissues lacking a cuticle to enable gas exchange when incubated in 25 mL glass vials with a solution of 10 % artificial lake water (see 'Plant material'). For P_N measurements, approx. 25 mg fresh mass (FM) of fully expanded leaves was incubated for about 2 h in a solution with O_2 initially at half air equilibrium to reduce the possibility of photorespiration (Setter *et al.*, 1989) and the amount of free CO_2 was either 200 or <2 mmol m^{-3} (see Pedersen *et al.*, 2013 for details on preparation). The transparent glass vials holding the leaf samples contained two glass beads and were rotated on a vertical wheel immersed in a constant temperature bath (20 °C) and illuminated with a LEP lamp (PRO LEP 300, Gavita, Aalsmeer, The Netherlands), providing a photon flux density of 250 µmol photons m^{-2} s^{-1}. After incubation, O_2 evolution was measured using an O_2 optode (OP-MR, Unisense); vials prepared in the same way but without tissues served as blanks. Finally, the FM of the leaf sample was measured to enable calculation of P_N with the units of nmol O_2 g^{-1} FM s^{-1}.

Underwater R_D was measured as O_2 consumption of leaf segments incubated in darkness. In brief, approx. 100 mg FM of fully expanded leaves (n = 4; green tissues only, excised and sliced longitudinally, see above) were incubated towards the end of the light period for about 3 h in a solution initially at near air equilibrium of O_2. After incubation (in glass vials but in the dark on the rotating wheel at 20 °C; see above), O_2 consumption was measured as described above, and FM was recorded to enable calculation of R_D with the units of nmol O_2 g^{-1} FM s^{-1}.

Sediment characteristics

Sediment organic matter was measured in the upper 3 cm representing the depth horizon in which measurements of dissolved CO_2 and O_2 were taken. A sediment core was taken with a Perspex cylinder (Ø = 46 mm) and the upper 3 cm was homogenized by mixing with a spoon, after which 1.75 cm^3 was transferred into a 10 mL porcelain cup and dried until constant weight at 65 °C. The samples (n = 5 representing five different cores) were then weighed (w_0) and transferred to a furnace at 550 °C for 6 h, after which they were weighed again (w_1). Organic matter was calculated as $(w_0 - w_1)/w_0$ and expressed as a percentage.

Biological O_2 consumption of the sediment sampled at the same depth horizon and homogenized as described above was measured by transferring a 1.75 cm^3 sample into a 25 mL glass vial also with approx. 10 mL of 10 % artificial lake water (see 'Plant material') added and the samples (n = 5 representing five different cores) were bubbled with air for 6 h to remove any chemical O_2 demand (Pulido *et al.*, 2011). Then, the vials were topped up with 10 % artificial lake water at near air equilibrium and two glass beads were added to promote mixing as the vials rotated on the incubator in darkness at 20 °C for about 20 h, after which the O_2 concentration was measured (see 'Underwater photosynthesis and dark respiration'). Vials with no sediment added served as blanks. Sediment O_2 consumption rates were calculated as nmol O_2 L^{-1} sediment s^{-1}.

Data analysis

Graphpad Prism 7.0 was used to prepare figures and to carry out relevant statistical analyses. In the tables and figures, the means ± s.e. are provided, and a significance level of 0.05 is used for all means comparison tests. The type of test used and the results of the analyses are provided in the figure legends and the table footnotes.

RESULTS

Contrasting pCO_2 and pO_2 dynamics in C_3 and CAM tissues in light/dark periods

The aquatic plants were completely submerged and had no functional stomata, so any changes in tissue pCO_2 would be due to photosynthesis and respiration processes with influence also from CO_2 entry via the root system from the sediment.

Lobelia dortmanna (C_3) and *Littorella uniflora* (CAM) showed contrasting tissue CO_2 dynamics in both light and darkness. Leaf tissue pCO_2 of *Lobelia dortmanna* steeply increased immediately after the light was switched off following a concave function, exceeded 1.0 kPa after only 25 min in darkness (Fig. 2A) and reached a quasi-steady state of approx. 2.5–3.5 kPa (Table 1). The depletion following onset of light was similarly dynamic and, in the example shown in Fig. 2A, tissue pCO_2 declined from 3.6 to 0.7 kPa in just 30 min, and within a few hours a new quasi-steady state was below the detection limit (0.001 kPa). In stark contrast to the C_3 plant, leaf tissue pCO_2 of *Littorella uniflora* (CAM) fluctuated in a characteristic manner in the dark period. Immediately after the onset of darkness, tissue pCO_2 increased but then soon declined again, so that pCO_2 'peaked' at a much lower level than for the C_3 plant; this initial peak was at most 0.16 kPa and CO_2 had begun to decline again after only 20–25 min of darkness (Figs 2B, and 3A, B).

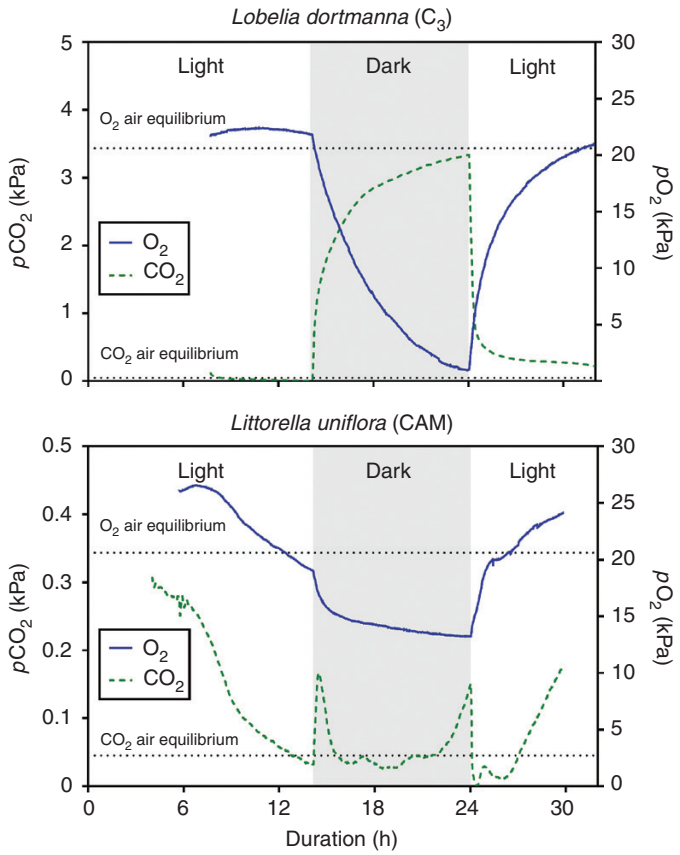

FIG. 2. Dynamics of CO_2 and O_2 partial pressures in the leaf lacunae of *Lobelia dortmanna* [C_3 photosynthesis (A)] and *Littorella uniflora* [CAM photosynthesis (B)] in a 14 h light and 10 h dark cycle. The CO_2 and O_2 microsensors were inserted into the youngest fully expanded leaf approx. 10–20 mm from the leaf tip <1 mm apart from each other. Measurements were at 20 °C with the water column maintained at near air equilibrium of both CO_2 (16 mmol m^{-3}) and O_2 (284 mmol m^{-3}), and with a constant flow velocity of approx. 1–2 mm s^{-1}. The plants were growing in a natural turf with a mixed community of *L. dortmanna* and *L. uniflora*; in light, the turf was illuminated with approx. 200 µmol photons m^{-2} s^{-1} at canopy height. Note the 10-fold difference in scale on the left *y*-axes (pCO_2); examples of other replicate plants are shown in Supplementary Data Fig. S1.

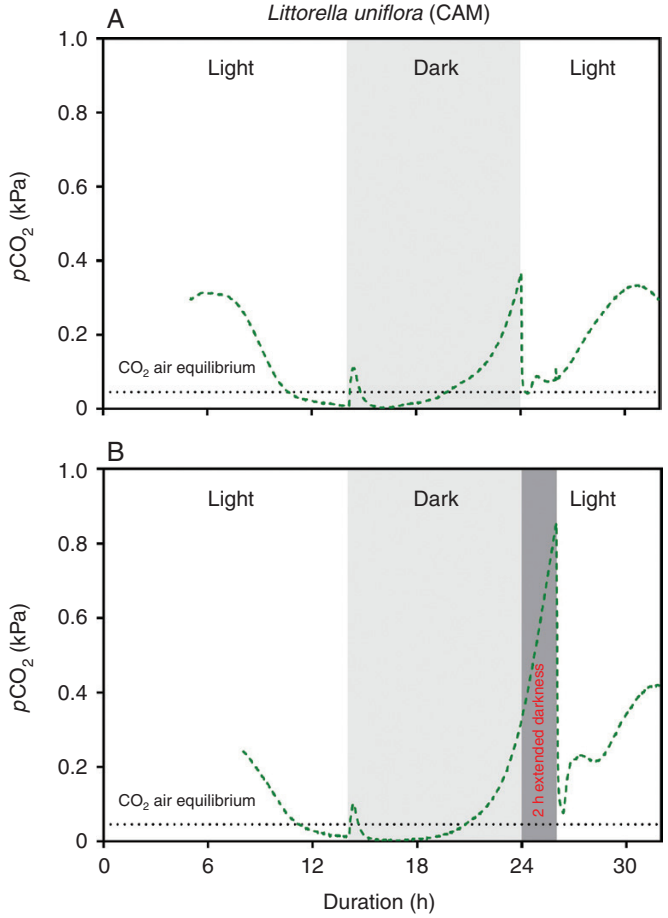

FIG. 3. Dynamics in CO_2 partial pressures in the leaf of *Littorella uniflora* (CAM photosynthesis) in a 14 h light and 10 h dark cycle (A) or 12 h light and 12 h dark cycle (B). The CO_2 microsensor was inserted into the youngest fully expanded leaf approx. 10–20 mm from the leaf tip. Measurements were at 20 °C with the water column maintained at near air equilibrium of both CO_2 (16 mmol m^{-3}) and O_2 (284 mmol m^{-3}) and with a constant flow velocity of about 1–2 mm s^{-1}. The plants were growing in a natural turf with a mixed community of *Lobelia dortmanna* and *Littorella uniflora*; in light, the turf was illuminated with approx. 200 µmol photons m^{-2} s^{-1} at canopy height.

Leaf tissue pCO_2 remained low, being below air equilibrium and sometimes even below the detection limit of 0.001 kPa for 4–6 h in the dark, before starting to increase slowly again following a convex function. When the light was switched on, tissue pCO_2 of the CAM plant declined from 0.15–0.37 kPa to very low levels in just 5–7 min (Figs 2B and 3A). After 1–1.5 h in the light, tissue pCO_2 increased steadily and on occasion reached 0.4 kPa before again declining towards the end of the light period (Figs 2B and 3A, B).

The observation that leaf tissue pCO_2 in *Littorella uniflora* (CAM) started to increase towards the end of the dark period prompted us to manipulate the duration of the dark period. Figure 3B shows the result of an extended dark period of 2 h and here leaf tissue pCO_2 continued to follow the convex-shaped increase already initiated during the last few hours of the dark period in the replicates shown in Figs 2B and 3A. Tissue pCO_2 rose from 0.31 to 0.85 kPa over a period of 2 h, but still declined steeply when the light was switched on (from 0.85 to 0.07 kPa in 20 min; Fig. 3B).

Leaf tissue pO_2 dynamics in *Lobelia dortmanna* largely followed the opposite pattern of that for pCO_2 in its tissues; pO_2 was slightly above air equilibrium at the end of the light period and then declined throughout the entire dark period without reaching a new quasi-steady state so that the leaf tissues were severely hypoxic (approx. 1 kPa) towards the end of the dark period (Fig. 1A; Table 1; Supplementary Data Fig. S1A). Leaf tissue pO_2 in *Littorella uniflora* (CAM) followed a pattern somewhat different from that of *Lobelia dortmanna* (C_3). *Littorella uniflora* maintained substantially higher O_2 status in the leaves during darkness, and tissue pO_2 levelled out at a quasi-steady state at 10–15 kPa. Tissue pO_2 increased steeply at the onset of light but, halfway into the light period, tissue pO_2 started declining (Fig. 2B; Supplementary Data Fig. S1B) and in one instance even declined to below air equilibrium (Fig. 2B).

Tissue concentrations of malate and citrate, and underwater net photosynthesis

The detailed time traces of internal pCO_2 of *Littorella uniflora* indicated CAM activity since leaf tissue pCO_2 was low in darkness and relatively high in the light. Therefore, since CAM involves night-time synthesis of organic acids which are subsequently decarboxylated the following day (Lüttge, 2004), we analysed leaf tissues of *Littorella uniflora* (CAM) and also of *Lobelia dortmanna* (C_3) for malate and citrate at the end of the dark and light periods. As expected, *Lobelia dortmanna* (C_3) had low levels of both malate and citrate and the tissue concentrations did not differ between the two time points (Fig. 4A, B). In contrast, leaf tissues of *Littorella uniflora* (CAM) showed high accumulation of malate in the dark period and a significant depletion of the malate pool during the light period (Fig. 4A). The dark fixation of CO_2 into malate by *Littorella uniflora* supports the observation of very low tissue pCO_2 throughout most of the dark period, and the depletion, i.e. decarboxylation, of the malate pool during the light similarly supports the relatively high tissue pCO_2 during the light period (Fig. 3A, B). Citrate concentration in the leaf tissue of *Littorella uniflora* was also considerably higher than in *Lobelia dortmanna*, but with no significant differences between the two sampling times (Fig. 4B).

Underwater P_N and R_D by leaf tissues of both *Lobelia dortmanna* (C_3) and *Littorella uniflora* (CAM) were measured using excised leaf tissues in closed glass vials. The rates of P_N did not differ for leaves sampled and measured at the end of the dark or light periods when 200 mmol CO_2 m^{-3} was provided, either for *Lobelia dortmanna* or for *Littorella uniflora* (Fig. 4D). The benefit of CAM over C_3 photosynthesis was, however, evident for measurements of P_N at low external CO_2 (<2 mmol m^{-3}). Leaf tissues of *Littorella uniflora* sampled at the end of the dark period (i.e. high in malate) and incubated at <2 mmol CO_2 m^{-3} had 4.7-fold higher rates of underwater P_N compared with *Lobelia dortmanna*, demonstrating the capacity for CAM to sustain P_N when external CO_2 is scarce (Fig. 4C). R_D of leaf tissues did not differ between the two species (0.609 ± 0.050 and 0.792 ± 0.098 µmol O_2 g^{-1} FM s^{-1} for *Lobelia dortmanna* and *Littorella uniflora*, respectively, mean ± s.e., $n = 4$).

Sediment CO_2 and O_2 dynamics

It is known that both *Lobelia dortmanna* and *Littorella uniflora* utilize sediment-derived CO_2 for photosynthesis and lose most of the O_2 produced to the sediment via root ROL (Sand-Jensen *et al.*, 1982; Madsen, 1985). Therefore, we followed

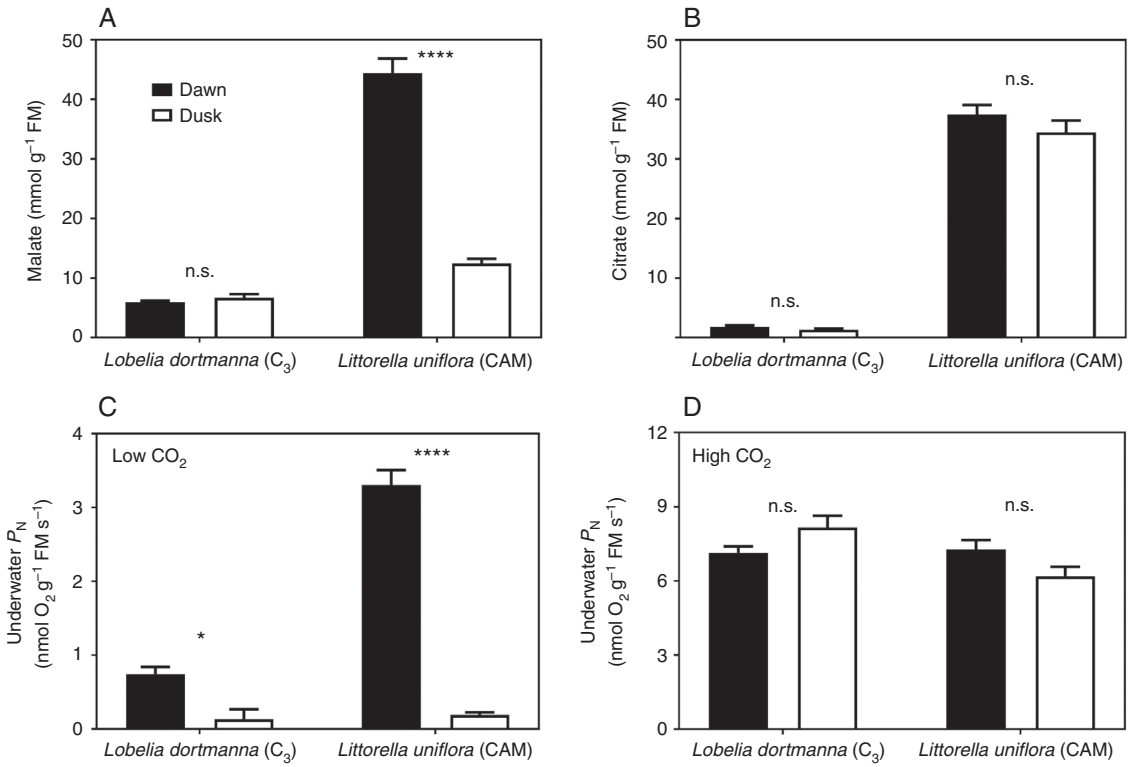

FIG. 4. Leaf tissue organic acids (A and B) and underwater net photosynthesis (P_N; C and D) of *Lobelia dortmanna* (C_3 photosynthesis) and *Littorella uniflora* (CAM photosynthesis) sampled at dawn (end of the 10 h dark period) or dusk (end of the 14 h light period). The plants were growing in a natural turf with a mixed community of *L. dortmanna* and *L. uniflora*; in light, the turf was illuminated with approx. 200 µmol photons m^{-2} s^{-1} at canopy height. The turfs were kept at 20 °C with the water column maintained at near air equilibrium of both CO_2 (16 mmol m^{-3}) and O_2 (284 mmol m^{-3}) and with a constant flow velocity of about 1–2 mm s^{-1}. Underwater P_N was measured as O_2 production at 250 µmol photons m^{-2} s^{-1} at low external CO_2 (<2 mmol m^{-3}) or high external CO_2 (approx. 250 mmol m^{-3}); note that vertical scales differ in (C) and (D). Data shown are the mean ± s.e. ($n = 5$ with each replicate representating all leaves in one individual plant for organic acids or the youngest fully expanded leaf for underwater P_N); asterisks denote a statistically significant difference (*$P < 0.05$ or ****0.0001, respectively; Tukey test) and n.s. = not significant.

CO_2 and O_2 dissolved in the porewater over a diel period at a depth with high root density of both species.

The highly permeable roots of the two species, together with the P_N in their shoots during the light period consuming CO_2 and producing O_2 and connected via aerenchyma to the roots, led to pronounced diel fluctuations in sediment CO_2 and O_2. In light, porewater pCO_2 was depleted from a quasi-steady state level of approx. 5 kPa at 'dawn' to approx. 2 kPa (Table 1, Fig. 5A, B); this substantial decline indicates CO_2 movement into the roots of the two isoetids which would result from the concentration gradient towards the photosynthetically active shoot. In darkness, porewater pCO_2 again increased steeply above that at the end of the light period and it levelled out at about 5 kPa. In contrast to pCO_2, porewater pO_2 followed an opposite pattern of changes in the light/dark cycle, showing a steep increase at the onset of light from approx. 0–10 kPa to approx. 8–18 kPa within 6–8 h, and as expected porewater pO_2 declined in darkness to a new quasi-steady state that sometimes fell below the detection limit (0.007 kPa) but in some other instances levelled out at about 10 kPa (Fig. 5A, B; Table 1; Supplementary Data Fig. S2). Interestingly, the shape of the sediment time traces of pO_2 did not always follow the exact opposite pattern of CO_2 but started to decline well before the onset of darkness (Fig. 5A, B) as also observed in the spongy leaf tissues of *Littorella uniflora* (Fig. 2B).

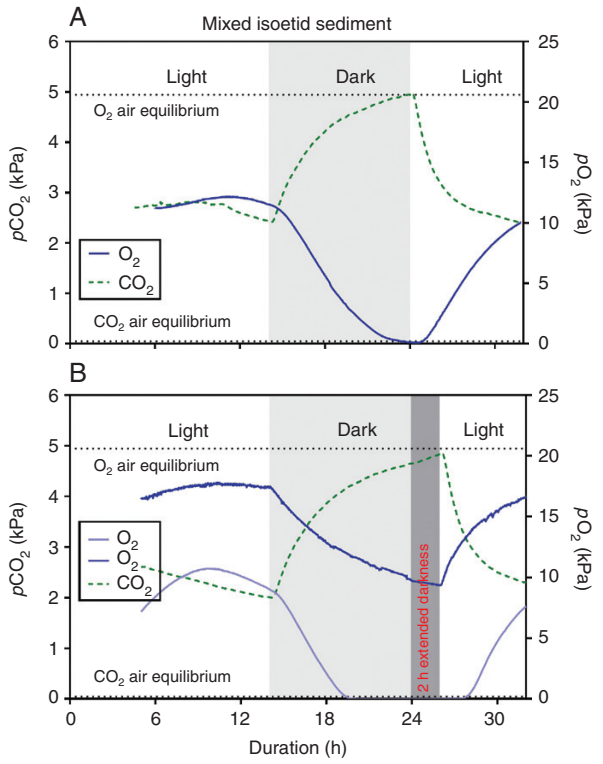

FIG. 5. Dynamics of CO_2 and O_2 partial pressures in the sediment inhabited by *Lobelia dortmanna* and *Littorella uniflora* kept in a 14 h light and 10 h dark cycle (A) or a 12 h light and 12 h dark cycle (B) but here with two oxygen traces showing different values but overall similar in pattern. The CO_2 and O_2 microsensors were inserted 3 cm into the sediment half way between two neighbouring plants. Measurements were at 20 °C with the water column maintained at near air equilibrium of both CO_2 (16 mmol m^{-3}) and O_2 (284 mmol m^{-3}) and with a constant flow velocity of approx. 1–2 mm s^{-1}. The plants were growing in a natural turf with a mixed community of *L. dortmanna* and *L. uniflora*; in light, the turf was illuminated with approx. 200 µmol photons m^{-2} s^{-1} at canopy height. The same data and additional replicates expressed in porewater concentration units of CO_2 and O_2 are shown in Supplementary Data Fig. S2.

DISCUSSION

The combined application of microsensors for CO_2 and O_2 enabled unparalleled temporal resolution of intratissue pCO_2 and pO_2 dynamics within leaves of intact plants, and revealed stark contrasts between the C_3 and CAM aquatic plants. For the C_3 plant, the CO_2 concentration increased throughout the dark period, whereas for the CAM plant internal CO_2 remained relatively low for most of the dark period, which would be due to the sequestration of CO_2 into malate. Moreover, the high temporal resolution elucidated an initial small peak (initial rise with subsequent decline) in pCO_2 following the onset of darkness then declining to an apparent quasi-steady state for several hours, followed again by increasing pCO_2 towards the end of the dark period which, respectively, indicate an initiation and then slowing of malate synthesis. During the light period, leaf pCO_2 was initially higher in the C_3 plant and steeply declined with photosynthesis, whereas in the CAM plant leaf pCO_2 was initially lower than in the C_3 plant but after an initial steep decline then remained relatively more steady than in the C_3 plant. Below, we discuss these findings, including the substantial temporal changes, as well as interspecies differences, in leaf tissue pCO_2 and pO_2 in the light–dark cycles. We also consider the dynamics of dissolved CO_2 and O_2 in the vegetated sediment.

Simultaneous direct measurements of pCO_2 and pO_2 in leaf tissues are rare and have previously been achieved by extraction of gases with syringes at discrete times, with subsequent analysis using GC. In the context of CAM physiology, such data were available for some terrestrial CAM species with succulent tissues. In *Sedum praealtum*, leaf tissue pO_2 remained constant throughout the dark period at around 20.6 kPa and then increased rapidly in light to 25 kPa before declining again as the internal pCO_2 was depleted from approx. 0.35 kPa down to 0.04 kPa at the end of the light period (Spalding *et al.*, 1979). Similarly following decarboxylation of malate soon after the onset of the light period, pCO_2 increased to 0.8 kPa in *Agave desertii* and to 2.4 kPa in *Opuntia basilaris*, and then declined towards the end of the light period as the malate pool became depleted (Cockburn *et al.*, 1979). For the aquatic CAM plant *Littorella uniflora* in the present study, following the switch from light to darkness, the leaf tissue pCO_2 exhibited an initial small peak (Figs 2B and 3A, B; Supplementary Data Fig. S1B), whereas for the earlier studied terrestrial CAM species an initial peak in tissue pCO_2 was poorly resolved for *A. dersertii* (Cockburn *et al.*, 1979) and was not observed for *S. praealtum* (Spalding *et al.*, 1979), possibly because of poor time resolution of the discrete samplings necessary in those earlier studies. Moreover, and unlike *Littorella uniflora*, the shoot tissues of the terrestrial species would not have had a continuous influx via the roots of sediment-derived CO_2 which occurs at a much higher concentration in soil than the pCO_2 in air (reviewed, for example, by Greenway *et al.*, 2006). The newly revealed dynamics in tissue pCO_2 for *L. uniflora* in the context of CAM physiology are further considered later in this Discussion.

Leaf pO_2 of *Lobelia dortmanna* increased from severely hypoxic values (approx. 1 kPa) late in the dark period to a new quasi-steady state level of about 21 kPa in the second half of the light period (Fig. 2A; Table 1). As we hypothesized for the C_3 *L. dortmanna*, pCO_2 in leaves declined rapidly immediately after the transition from darkness to light, and in some cases leaf tissue pCO_2 remained below the detection limit for hours (Fig. 2A; Supplementary Data Fig. S1A). However, since tissue pO_2 remained relatively constant during the last several hours of the light period, P_N must have been fuelled by a steady flux of sediment-derived CO_2. This notion is supported by substantial declines in sediment pCO_2 during the light period (Fig. 5A, B; Pedersen *et al.*, 1995; Lenzewski *et al.*, 2018) at a sediment depth where root density is high (Pedersen *et al.*, 1995). The entry of sediment-derived CO_2 and its diffusion to the shoots, thus fuelling P_N, results in rising tissue pO_2 (Fig. 2A, B; Supplementary Data Fig. S1A, B) and therefore increased root ROL to the sediment, leading to increases in sediment pO_2 within the rooting zone, a general phenomenon in isoetid-inhabited sediments (Møller and Sand-Jensen, 2011, 2012; Pedersen *et al.*, 2011*a*; Lenzewski *et al.*, 2018). The pO_2 in sediments varied amongst replicates, presumably as a result of differences in plant density and distance between the sensor tip and the nearest root and thus source of O_2 (Fig. 5; Supplementary Data Fig. S2). The dynamic nature of gaseous O_2 in the leaf lacunae of *L. dortmanna* had previously been shown in laboratory cultures as well as in a field situation (Møller and Sand-Jensen, 2011; Sand-Jensen *et al.*, 2005), and internal pO_2 also in these studies levelled out during the light period, indicating a balance between O_2 production from P_N as determined by CO_2 supply, and O_2 consumed in respiration or lost to the sediment via root ROL during this quasi-steady state for this C_3 aquatic species.

Interestingly, leaf tissue pO_2 dynamics of *Littorella uniflora* (CAM) followed a very different pattern from those of *Lobelia dortmanna* (C_3; see preceding paragraph). First, leaf pO_2 in darkness never declined to critically low levels (Fig. 2B; Supplementary Data Fig. S1B) and this is likely to be due to the higher cuticle permeability to O_2 in *Littorella uniflora* compared with that of *Lobelia dortmanna* (Møller and Sand-Jensen, 2012) so that O_2 from the surrounding water can enter *Littorella uniflora* and sustain leaf and root respiration in the dark. During the first several hours in the light period, tissue pO_2 was higher in *Littorella uniflora* than in the C_3 plant; the decarboxylations of the malate pool enabled greater tissue pCO_2 (up to 10-fold air equilibrium) to fuel P_N and thus produce O_2. However, leaf tissue pO_2 of *Littorella uniflora* declined somewhat in the second half of the light period (Fig. 2B; Supplementary Data Fig. S1B), which differed from the pattern for the C_3 plant. Relative to the air equilibrium level, towards the end of the light period leaf pO_2 in *Littorella uniflora* showed a deficit of 2.6 kPa (Fig. 2B) or 0.6 kPa (Supplementary Data Fig. S1B) below this benchmark. Although these small differences in tissue pO_2 levels between the two phases in light would not be expected to impact on respiration, these declines in pO_2 are of interest as they are probably caused by CO_2 limitation of leaf P_N as indicated by parallel declines in leaf pCO_2 also towards the end of the light period (Fig. 2B; Supplementary Data Fig. S1B) as the malate pool is being depleted and the decarboxylation of malate must presumably be slowing down during this latter part of the light period (Fig. 4A). Internal pO_2 in *Littorella uniflora* declined during the second half of the light period when the malate pool has declined and the P_N becomes increasingly reliant on CO_2 entry from the sediment, since the root system of *Littorella uniflora* (CAM) is smaller than that of the C_3 *Lobelia dortmanna* (Fig. 1C, D), and so the CAM species would have a smaller flux of sediment-derived CO_2.

Leaf tissue CO_2 dynamics during darkness exhibited three distinct phases in the CAM isoetid

Leaf tissue pCO_2 measurements in submerged *Littorella uniflora* (CAM) revealed three distinct phases following the onset of darkness. An initial peak in pCO_2 (phase 1) following the cessation of P_N upon darkness probably results from a combination of the continued tissue respiration and the flux of sediment-derived CO_2 via the aerenchyma and an apparent lag in maximal phosphoenolpyruvate carboxylase (PEPc) activity, so that pCO_2 rises within the tissues. However, within 20–30 min, leaf tissue pCO_2 then declines and remains low for the hours of darkness (phase 2), indicating that CO_2 is fixed by PEPc to form malate. This period of several hours of malate synthesis and the resulting very low tissue pCO_2 is followed by transitions towards the end of the dark period to gradual increases in tissue pCO_2 (phase 3) which presumably results from a slowing down of malate synthesis. We can rule out that the low tissue pCO_2 observed in phase 2 is due to radial diffusional loss of CO_2 to the surrounding water facilitated by the more permeable leaf cuticle in *Littorella uniflora* compared with *Lobelia dortmanna* (Møller and Sand-Jensen, 2012) since this phase is characterized by low tissue pCO_2 (often below air equilibrium) so that any net flux of CO_2 would occur from the water and into the leaf tissues as the water is maintained at near air equilibrium in both light and darkness by purging with atmospheric air.

The present study with continuous monitoring of tissue pCO_2 in the CAM aquatic *Littorella uniflora* can be compared with knowledge of regulation of PEPc activity and malate synthesis in terrestrial CAM plants. The diel activity of PEPc in terrestrial CAM plants is mainly controlled by its phosphorylation state (Nimmo, 1998); when phosphorylated, the sensitivity to the allosteric inhibitor, malate, is 10-fold lower (Nimmo *et al.*, 1984). PEPc phosphorylation is controlled by PEPc kinase and, in *Mesembryanthemum crystallinum* (Taybi *et al.*, 2000) and *Kalanchoe fedtschenkoi* (Hartwell *et al.*, 1999), the transcript abundance of PEPc kinase is regulated by a 'circadian oscillator' and not by simple light–dark transitions (Nimmo *et al.*, 1987). In the case of *Kalanchoe fedtschenkoi*, conversions of PEPc sensitivity to malate occurred during the dark period, about 4 h after the lights went off (to the malate-insensitive form) and about 2 h before the lights came back on (to the malate-sensitive form) (8 h light, 16 h dark; Nimmo *et al.*, 1984). Considering now the pCO_2 dynamics for the CAM aquatic *Littorella uniflora*, the initial small rise and then swift decline in leaf tissue pCO_2 following the onset of darkness (phase 1) indicates that significant malate synthesis had commenced 20–30 min into the dark period, so that: (*a*) the malate produced must be efficiently compartmentalized away from the PEPc; and/

or (*b*) timing of the regulation of the phosphorylation state of PEPc may be different in *Littorella uniflora* from that reported by Nimmo *et al.* (1984) for *K. fedtschenkoi*. Turning now to near the end of the dark period, the increases in tissue pCO_2 indicate that malate synthesis had slowed (phase 3), since respiration and flux of sediment-derived CO_2 would both continue; the extended dark period during which tissue pCO_2 continues to rise is in accordance with the proposed mechanism (Fig. 3B). If the phosphorylation state of PEPc in the CAM aquatic *Littorella uniflora* also declines towards the end of the night, as reported for *K. fedtschenkoi* (Nimmo *et al.*, 1984), then malate synthesis would slow down. Thus, the high temporal resolution monitoring of leaf pCO_2 has revealed these distinct phases of CAM metabolism during the dark period.

The distinct dynamics during the dark period of leaf pCO_2 in the CAM *Littorella uniflora*, owing to influx of CO_2 from the sediments and apparent changes in activity of CO_2 sequestration to malate as part of CAM metabolism (described above), contrasts with the continued increase in leaf pCO_2 in the C_3 *Lobelia dortmanna* for which the rate of increase in leaf pCO_2 declined as the concentration gradient from sediment to leaf also decreased as leaf pCO_2 approached up to 3.5 kPa. The consequences for the underwater photosynthesis by these C_3 and CAM isoetids are discussed in the next section, and the influence on daytime pO_2 dynamics in the plant and sediments was considered earlier in this Discussion.

Comparison of rates of underwater photosynthesis (P_N) in the C_3 and CAM isoetids

The benefit of CAM in *Littorella uniflora* was evident in the data on underwater P_N. Leaf tissues of *L. uniflora* sampled at the end of the dark period showed significantly higher rates of P_N compared with leaves from the C_3 plant but only when external CO_2 supply was low and limiting (Fig. 4C); high external CO_2 masked the benefit of CAM (Fig. 4D). This finding confirms previous studies of *L. uniflora* and other aquatic CAM plants that strongly indicate that CAM is of benefit only when environmental CO_2 is scarce (Madsen, 1987; Keeley, 1998; Klavsen and Madsen, 2012). Interestingly, leaf tissues of *Lobelia dortmanna* (C_3) sampled at the end of the dark period also showed significantly higher rates of P_N compared with leaf tissues sampled at the end of the light period. This has not previously been shown for *L. dortmanna* and we suspect that the extremely high pCO_2 levels in the leaf lacunae at the end of the dark period leads to CO_2 accumulation in the tissue sap, and the dissolved CO_2 can then contribute to fuelling some P_N at least in the early hours. Putative build-up of respiratory CO_2 resulting in initially higher rates of P_N has previously been attributed as the cause of initial peaks in tissue pO_2 of submerged C_3 plants following sunrise (Pedersen *et al.*, 2006) or at transitions from darkness to light in laboratory experiments (Colmer and Pedersen, 2008). We can rule out any role for decarboxylation of malate or citrate in the enhanced P_N observed for *L. dortmanna* in the early morning hours, since in this C_3 species there were no significant changes between 'dawn' and 'dusk' in leaf tissue pools of these organic acids (Fig. 4A, B).

Conclusions

The new CO_2 microsensor has enabled unparalleled temporal resolution of tissue CO_2 dynamics, revealing stark contrasts between C_3 and CAM aquatic plants. Both species were of the isoetid life form that promotes use of sediment-derived CO_2. During darkness, shoot tissue pCO_2 increased up to 3.5 kPa in the C_3 species, whereas it remained below 0.05 kPa in the CAM species owing to sequestration of CO_2 into malate. The high temporal resolution of the CO_2 microsensor elucidated three phases of nocturnal CO_2 sequestration in the CAM species: (1) an initial lag of 20–30 min; (2) sequestration for several hours; and (3) a slow down of sequestration during the final hours of darkness. These contrasting CO_2 acquisition strategies influence underwater photosynthesis, which together with apparent differences in cuticle resistance determined tissue O_2 status that differed markedly between the two species during the dark period. The utility of the new CO_2 microsensor has been demonstrated, as applied to the physiology of aquatic species with contrasting carbon acquisition strategies. The new CO_2 microsensor will enable future laboratory studies testing additional hypotheses related to temporal patterns and spatial gradients of CO_2 in plant organs/tissues, and similarly to the use of O_2 microsensors in field situations to resolve questions related to plant aeration [e.g. rice (Winkel *et al.*, 2013)], deployment of the new CO_2 microsensor will enhance field studies of CAM and various other applications in plant ecophysiology.

SUPPLEMENTARY DATA

Supplementary data are available online at https://academic.oup.com/aob and consist of the following. Figure S1: CO_2 and O_2 dynamics in the leaf lacunae of *Lobelia dortmanna* (C_3 photosynthesis) and *Littorella uniflora* (CAM photosynthesis) in a 14 h light and 10 h dark cycle. Figure S2: CO_2 and O_2 dynamics in the sediment inhabited by *Lobelia dortmanna* and *Littorella uniflora* maintained in a 14 h light and 10 h dark cycle or 12 h light and 12 h dark.

ACKNOWLEDGEMENTS

We thank Gregory R. Cawthray for HPLC analyses of malate and citrate. Länsstyrelsen in Skåne Län is thanked for permission to sample isoetids in Värsjön. Lars Borregaard Pedersen is thanked for construction of microsensors used in this study. Acknowledgements of grants: O.P., the Villum Foundation VKR023382 and the Carlsberg Foundation CF15-0092; N.P.R., the EU Framework 7 Project 'Senseocean', grant no. 614141 and the Grundfos Foundation.

LITERATURE CITED

Armstrong W. 1964. Oxygen diffusion from the roots of some British bog plants. *Nature* **204**: 801–802.

Armstrong W. 1979. Aeration in higher plants. *Advances in Botanical Research* **7**: 225–332.

Caflisch CR, Solomon S, Galey WR. 1979. Exocrine ductal pCO_2 in the rabbit pancreas. *Pflügers Archiv* **380**: 121–125.

Clark LC Jr. 1956. Monitor and control of blood and tissue oxygen tensions. *Transactions of the American Society of Artificial Internal Organs* **2**: 41–48.

Cockburn W, **Ting IP**, **Sternberg LO. 1979**. Relationships between stomatal behavior and internal carbon dioxide concentration in Crassulacean acid metabolism plants. *Plant Physiology* **63**: 1029–1032.

Colmer TD. 2003. Long-distance transport of gases in plants: a perspective on internal aeration and radial oxygen loss from roots. *Plant, Cell and Environment* **26**: 17–36.

Colmer TD, **Pedersen O. 2008**. Oxygen dynamics in submerged rice (*Oryza sativa*). *New Phytologist* **178**: 326–334.

De Beer D, **Glud A**, **Epping E**, **Kuhl M. 1997**. A fast-responding CO_2 microelectrode for profiling sediments, microbial mats, and biofilms. *Limnology and Oceanography* **42**: 1590–1600.

Fan TWM, **Colmer TD**, **Lane AN**, **Higashi RM. 1993**. Determination of metabolites by ^{1}H NMR and GC: analysis for organic osmolytes in crude tissue extracts. *Analytical Biochemistry* **214**: 260–271.

Farmer AM, **Spence DHN. 1985**. Studies of diurnal acid fluctuations in British isoetid-type submerged aquatic macrophytes. *Annals of Botany* **56**: 347–350.

Greenway H, **Armstrong W**, **Colmer TD. 2006**. Conditions leading to high CO_2 (>5 kPa) in waterlogged–flooded soils and possible effects on root growth and metabolism. *Annals of Botany* **98**: 9–32.

Hartwell J, **Gill A**, **Nimmo GA**, **Wilkins MB**, **Jenkins GI**, **Nimmo HG. 1999**. Phosphoenolpyruvate carboxylase kinase is a novel protein kinase regulated at the level of expression. *The Plant Journal* **20**: 333–342.

Hutchinson GE. 1975. *A treatise on limnology. Volume III. Limnological botany*. New York: John Wiley & Sons, Inc.

Keeley JE. 1998. CAM photosynthesis in submerged aquatic plants. *Botanical Review* **64**: 121–175.

Keeley JE, **Busch G. 1984**. Carbon assimilation characteristics of the aquatic CAM plant, *Isoetes howellii*. *Plant Physiology* **76**: 525–530.

Klavsen S, **Madsen T. 2012**. Seasonal variation in crassulacean acid metabolism by the aquatic isoetid *Littorella uniflora*. *Photosynthesis Research* **112**: 163–173.

Kluge M, **Böhlke C**, **Queiroz O. 1981**. Crassulacean acid metabolism (CAM) in *Kalanchoë*: changes in intercellular CO_2 concentration during a normal CAM cycle and during cycles in continuous light or darkness. *Planta* **152**: 87–92.

Lenzewski N, **Mueller P**, **Meier RJ**, **Liebsch G**, **Jensen K**, **Koop-Jakobsen K. 2018**. Dynamics of oxygen and carbon dioxide in rhizospheres of *Lobelia dortmanna* – a planar optode study of belowground gas exchange between plants and sediment. *New Phytologist* **218**: 131–141.

Long SP, **Bernacchi CJ. 2003**. Gas exchange measurements, what can they tell us about the underlying limitations to photosynthesis? Procedures and sources of error. *Journal of Experimental Botany* **54**: 2393–2401.

Lüttge U. 2004. Ecophysiology of Crassulacean acid metabolism (CAM). *Annals of Botany* **93**: 629–652.

Maberly SC, **Spence DHN. 1983**. Photosynthetic inorganic carbon use by freshwater plants. *Journal of Ecology* **71**: 705–724.

Madsen TV. 1985. A community of submerged aquatic CAM plants in Lake Kalgaard, Denmark. *Aquatic Botany* **23**: 97–108.

Madsen TV. 1987. Sources of inorganic carbon acquired through CAM in *Littorella uniflora* (L.) Aschers. *Journal of Experimental Botany* **38**: 367–377.

Madsen TV, **Sand-Jensen K. 1991**. Photosynthetic carbon assimilation in aquatic macrophytes. *Aquatic Botany* **41**: 5–40.

Møller CL, **Sand-Jensen K. 2011**. High sensitivity of *Lobelia dortmanna* to sediment oxygen depletion following organic enrichment. *New Phytologist* **190**: 320–331.

Møller CL, **Sand-Jensen K. 2012**. Rapid oxygen exchange across the leaves of *Littorella uniflora* provides tolerance to sediment anoxia. *Freshwater Biology* **57**: 1875–1883.

Nimmo GA, **Nimmo HG**, **Fewson CA**, **Wilkins MB. 1984**. Diurnal changes in the properties of phosphoenolpyruvate carboxylase in *Bryophyllum* leaves: a possible covalent modification. *FEBS Letters* **178**: 199–203.

Nimmo GA, **Wilkins MB**, **Fewson CA**, **Nimmo HG. 1987**. Persistent circadian rhythms in the phosphorylation state of phosphoenolpyruvate carboxylase from *Bryophyllum fedtschenkoi* leaves and in its sensitivity to inhibition by malate. *Planta* **170**: 408–415.

Nimmo HG. 1998. Circadian regulation of a plant protein kinase. *Chronobiology International* **15**: 109–118.

Pedersen O, **Sand-Jensen K. 1992**. Adaptations of submerged *Lobelia dortmanna* to aerial life form – morphology, carbon sources and oxygen dynamics. *Oikos* **65**: 89–96.

Pedersen O, **Sand-Jensen K**, **Revsbech NP. 1995**. Diel pulses of O_2 and CO_2 in sandy lake sediments inhabited by *Lobelia dortmanna*. *Ecology* **76**: 1536–1545.

Pedersen O, **Vos H**, **Colmer TD. 2006**. Oxygen dynamics during submergence in the halophytic stem succulent *Halosarcia pergranulata*. *Plant, Cell and Environment* **29**: 1388–1399.

Pedersen O, **Pulido C**, **Rich SM**, **Colmer TD. 2011*a***. *In situ* O_2 dynamics in submerged *Isoetes australis*: varied leaf gas permeability influences underwater photosynthesis and internal O_2. *Journal of Experimental Botany* **62**: 4691–4700.

Pedersen O, **Rich SM**, **Pulido C**, **Cawthray GR**, **Colmer TD. 2011*b***. Crassulacean acid metabolism enhances underwater photosynthesis and diminishes photorespiration in the aquatic plant *Isoetes australis*. *New Phytologist* **190**: 332–339.

Pedersen O, **Colmer TD**, **Sand-Jensen K. 2013**. Underwater photosynthesis of submerged plants – recent advances and methods. *Frontiers in Plant Science* **4**: 140. doi: 10.3389/fpls.2013.00140.

Pulido C, **Lucassen ECHET**, **Pedersen O**, **Roelofs JGM. 2011**. Influence of quantity and lability of sediment organic matter on the biomass of two isoetids, *Littorella uniflora* and *Echinodorus repens*. *Freshwater Biology* **56**: 939–951.

Raven JA, **Handley LL**, **MacFarlane JJ**, ***et al.* 1998**. The role of CO_2 uptake by roots and CAM in acquisition of inorganic C by plants of the isoetid life-form: a review, with new data on *Eriocaulon decangulare* L. *Philosophical Transactions of the Royal Society B: Biological Sciences* **363**: 2641–2650.

Revsbech NP. 1989. An oxygen microelectrode with a guard cathode. *Limnology and Oceanography* **34**: 474–478.

Sand-Jensen K, **Prahl C. 1982**. Oxygen-exchange with the lacunae and across leaves and roots of the submerged vascular macrophyte, *Lobelia dortmanna* L. *New Phytologist* **91**: 103–120.

Sand-Jensen K, **Prahl C**, **Stokholm H. 1982**. Oxygen release from roots of submerged aquatic macrophytes. *Oikos* **38**: 349–354.

Sand-Jensen K, **Pedersen O**, **Binzer T**, **Borum J. 2005**. Contrasting oxygen dynamics in the freshwater isoetid *Lobelia dortmanna* and the marine seagrass *Zostera marina*. *Annals of Botany* **96**: 613–623.

Sculthorpe CD. 1967. *The biology of aquatic vascular plants*. London: Edward Arnold Ltd.

Setter TL, **Waters I**, **Wallace I**, **Bekhasut P**, **Greenway H. 1989**. Submergence of rice. I. Growth and photosynthetic response to CO_2 enrichment of floodwater. *Australian Journal of Plant Physiology* **16**: 251–263.

Severinghaus JW, **Bradley AF. 1958**. Electrodes for blood pO_2 and pCO_2 determination. *Journal of Applied Physiology* **13**: 515–520.

Smart R, **Barko J. 1985**. Laboratory culture of submersed freshwater macrophytes on natural sediments. *Aquatic Botany* **21**: 251–263.

Spalding MH, **Stumpf DK**, **Ku MSB**, **Burris RH**, **Edwards GE. 1979**. Crassulacean acid metabolism and diurnal variations of internal CO_2 and O_2 concentrations in *Sedum praealtum* DC. *Functional Plant Biology* **6**: 557–567.

Taybi T, **Patil S**, **Chollet R**, **Cushman JC. 2000**. A minimal serine/threonine protein kinase circadianly regulates phosphoenolpyruvate carboxylase activity in crassulacean acid metabolism-induced leaves of the common ice plant. *Plant Physiology* **123**: 1471–1482.

Winkel A, **Colmer TD**, **Ismail AM**, **Pedersen O. 2013**. Internal aeration of paddy field rice (*Oryza sativa* L.) during complete submergence – importance of light and floodwater O_2. *New Phytologist* **197**: 1193–1203.

Wium-Andersen S. 1971. Photosynthetic uptake of free CO_2, by the roots of *Lobelia dortmanna*. *Physiologia Plantarum* **25**: 245–248.

Zhao P, **Cai W-J. 1997**. An improved potentiometric pCO_2 microelectrode. *Analytical Chemistry* **69**: 5052–5058.